


Article

Waterproof Aerated Bricks from Stone Powder Waste through Nano-TiO₂ Structured Hydrophobic Surface Modification

Tao Li ¹, Shaopeng Zeng ², Yaxiong Ji ³, Boxu Shen ³, Zhuangmiao Wang ⁴, Hong Zhong ^{3,*} and Shifeng Wang ^{5,*} ¹ School of Physics and Electrical Engineering, Qinghai Normal University, Xining 810000, China² Culver Academies, Culver, IN 46511, USA³ Department of Building Services Engineering, The Hong Kong Polytechnic University, Hong Kong 999077, China⁴ Department of Applied Physics, College of Sciences, Shanghai Institute of Technology, Shanghai 200000, China⁵ Department of Physics, College of Science, Tibet University, Lhasa 850000, China

* Correspondence: hzhong@polyu.edu.hk (H.Z.); wsf@utibet.edu.cn (S.W.)

Received: 24 May 2019; Accepted: 25 June 2019; Published: 28 June 2019



Abstract: To eliminate the negative impacts of waste stone powder that arises from stone processing, the waste was recycled into aerated bricks with a porous structure that exhibited exceptional properties when applied in buildings. However, the pores easily absorb rainwater and dust, causing performance degradation and mold growth inside. In this paper, we have developed through hydrothermal reactions an environmentally friendly aqueous suspension, containing homemade highly dispersive TiO₂ nanoparticles modified with super-hydrophobic groups on the surface. The suspension was coated onto the aerated bricks, creating a super-hydrophobic surface with a highly textured hierarchical structure. A large contact angle of 146° tested on the surface and negligible water absorption for 24 h immersion demonstrate the excellent water proofing performance, holding a great promise for large scale applications in construction and buildings.

Keywords: aerated brick; waste recycling; hydrophobic; surface modification; TiO₂ nanoparticle; highly dispersive

1. Introduction

Owing to the increasing demand for stone construction and decoration materials world wide because of the continuing growth in the world's population, a tremendous amount of stone powder waste has been generated in the natural and artificial stone industry during the cutting and carving processing stages, which could account for up to 35% of the weight of the stone that was used. The waste powder ranging from nanometers to millimeters is disposed of in landfills or arbitrarily discharged to the surrounding environment, and is prone to drift in air, which has not only caused severe environmental and ecological damage, but also carried risks to public health [1]. Fortunately, a growing awareness of these issues has been raised by both local municipal managers and many researchers from different fields.

Several methods have been adopted and implemented to recycle the waste stone powder. At present, the reuse strategies concentrate upon incorporating the stone byproduct as additives into the traditional construction materials, such as cement and concrete, to regulate their mechanical properties [2–5]. Other applications for reusing the stone powder have been developed by researchers in the area of functional nanomaterials, such as a self-cleaning coating based on waste marble [6],

or a marble powder derived paint for indoor air quality improvement [1]. However, the stone powder is reused as a type of auxiliary material, which consumes a pretty negligible amount of waste. Moreover, adding the stone powder into the products sometimes degrades the performances of the products. Recently, a recycling strategy of converting the waste stone powder into aerated bricks has gained considerable interest, since it makes full use of the stone powder as a main source for massive production, and has great application potential in the building and construction areas. Additionally, the manufacturing cost is relatively low.

The aerated brick made from the waste stone powder exhibits a porous structure, which leads to its exceptional properties, such as light weight, low bulk density, high heat resistance, excellent sound insulation, and small shrinkage [7,8]. However, it is precisely because of the pores that the aerated bricks easily absorb rainwater and suffer from water erosion, which degrades the mechanical and thermal performances and facilitates mold growth [8]. In order to solve the water invasion problem and maintain the edge of the aerated bricks, some reports have utilized rick husk ash to reduce the water absorption of the aerated bricks [9], or combined fly ash with silica to form dense matrixes for water resistance [10]. However, most of the above approaches make the manufacturing process more complicated and costly. Instead, creating hydrophobic surface by means of surface modification to achieve waterproof function would be more cost-effective and convenient for mass production. Inspired by the lotus leaf, a super-hydrophobic surface could be built through a highly textured epidermis layer combined with extremely low water affinity materials [6,11–15].

In this paper, an environmentally friendly aqueous based super-hydrophobic suspension was prepared, which contains homemade highly dispersed TiO_2 nanoparticles modified by super-hydrophobic groups deriving from perfluorooctyltriethoxysilane (PFOTS). The particle size of the nano- TiO_2 in anatase phase dispersed in water concentrates at about $0.28 \mu\text{m}$ with a relatively narrow distribution, indicating an extremely high degree of water dispersion. The aerated bricks were fabricated in a factory near the stone processing plants in Fujian Province, China, where our studies were conducted. Then the bricks were coated with the above suspension, creating a super-hydrophobic surface. A contact angle of 146° has been achieved on the modified surface of the aerated brick, demonstrating the excellent water repellency. Compared to a 55.1% increase in weight for the bare brick immersed in water for 24 h, the negligible water absorption in the brick with surface modification has proven the outstanding water proofing performance in practice. This super-hydrophobic surface modification enables the aerated bricks from stone powder waste recycling to possess strong water repellency ability, holding great promise for large scale applications in construction and buildings.

2. Materials and Methods

2.1. Fabrication of Aerated Bricks with Surface Modification

The recycling process from stone powder waste to aerated bricks was performed in Fengzhu Novel Construction Materials Co., LTD in Fujian Province, China. The stone waste was firstly milled by using a ball grinder, and then pumped to a slurry tank. Then lime, concrete, sand, and foaming agent were added at an appropriate ratio into the tank, followed by stirring with water. The slurry was then introduced into the injection molds and delivered to a still kettle after solidification. Under steam curing in the still kettle, porous aerated bricks were produced.

In this study, the aerated brick surface was coated with a novel homemade self-dispersed TiO_2 nanoparticle to form the hydrophobic hierarchical double structure. The TiO_2 particles were synthesized through a controllable hydrothermal reaction, as described in our previous studies [1,6,16]. In this research, firstly, 5 g of TiO_2 nanoparticles were dispersed into 20 ml of a mixture solution of water and ethylene glycol (purchased from Sigma-Aldrich) at a ratio of 1:1. Then, 0.8 wt.% of 1H,1H,2H,2H- perfluorooctyltriethoxysilane (PFOTS, purchased from Nanjing Quanxi Chemical Co., LTD, China) and 2 wt.% of tetraethoxysilane (TEOS, purchased from Aladdin, China) were added into the mixture under a stirring condition at a speed of 500 r/min. After another 2 h of continuous stirring,

a super-hydrophobic suspension could be obtained. Finally, the hydrophobic surface of the aerated bricks was achieved through dip coating or spray method.

2.2. Characterizations

The crystal phases of the samples were investigated by X-ray diffraction (XRD) using a Rigaku Smartlab 9 kW X-ray diffractometer, equipped with a $\text{Cu-K}\alpha_1$ radiation source ($\lambda = 1.5406 \text{ \AA}$). The microstructure of the materials was visualized using scanning electron microscopy (SEM) by employing a JEOL 6490 microscope at an accelerating voltage of 20 kV, while the elemental analysis of the samples was examined by using an energy dispersive spectrometer (EDS), which is attached to the JEOL 6490 microscope. Atomic force microscopy (AFM) was utilized to survey the surface morphology of the samples, which was performed on a Bruker NanoScope 8 in tapping mode using a silicon cantilever with a tip radius of less than 10 nm and resonance frequency of 278 kHz. The mean particle size and the width of the particle distribution of the prepared TiO_2 nanoparticles dispersed in deionized water were determined by using a Malvern Mastersizer 3000 laser particle size analyzer. Fourier transform infrared spectroscopy (FT-IR) measurements were carried out to examine the atomic bonding in the prepared coating by using a Bruker Vertex-70 spectrometer, and the absorption spectra were collected in the range of $400\text{--}1400 \text{ cm}^{-1}$ applying a spectral resolution of 2 cm^{-1} . The surface wettability of the modified aerated brick was quantified by the contact angle, which was performed on a PowerEach JC2000D contact angle meter using the 5-point fitting method with a droplet volume of $2 \mu\text{L}$.

3. Results and Discussion

The stone powder is mainly composed of silicon dioxide, calcium carbonate, and other aluminum silicate containing calcium [17], which is identified by XRD measurement shown in the lower red curve in Figure 1 and EDS element detection presented in Table S1 in the Supplementary Materials. The stone powder was mixed with concrete and sand, and then fabricated into aerated bricks. As displayed in Figure 1, an approximate coincidence of diffraction peaks between the two curves confirms that the composition of aerated brick is nearly the same as that of the waste stone powder. The unchanged composition from waste stone powder to aerated bricks was also verified by comparison of the chemical elements employing EDS, which is shown in Figure S1, Table S1 and Table S2 in the Supplementary Materials.

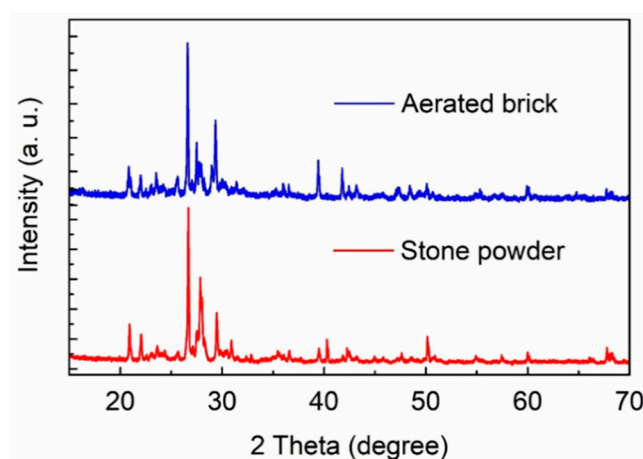


Figure 1. XRD patterns of the waste stone powder (lower red curve) and the aerated brick (upper blue curve).

Figure 2 shows the microstructure and morphology of the fabricated aerated brick visualized by using SEM at different magnifications. It is observed that the aerated brick is composed of flakes with a diameter of several micrometers and a thickness of hundreds of nanometers, being cross-linked and

exhibiting a porous structure with the pore size on the micrometer scale. This porous structure enables the aerated brick to possess outstanding properties such as good thermal shielding, sound insulation, light weight, and large pressure tolerance. However, the pores, in turn, could also easily absorb water from rains, consequently facilitating mold growth, suffering from corrosion, and degrading the performances of the bricks.

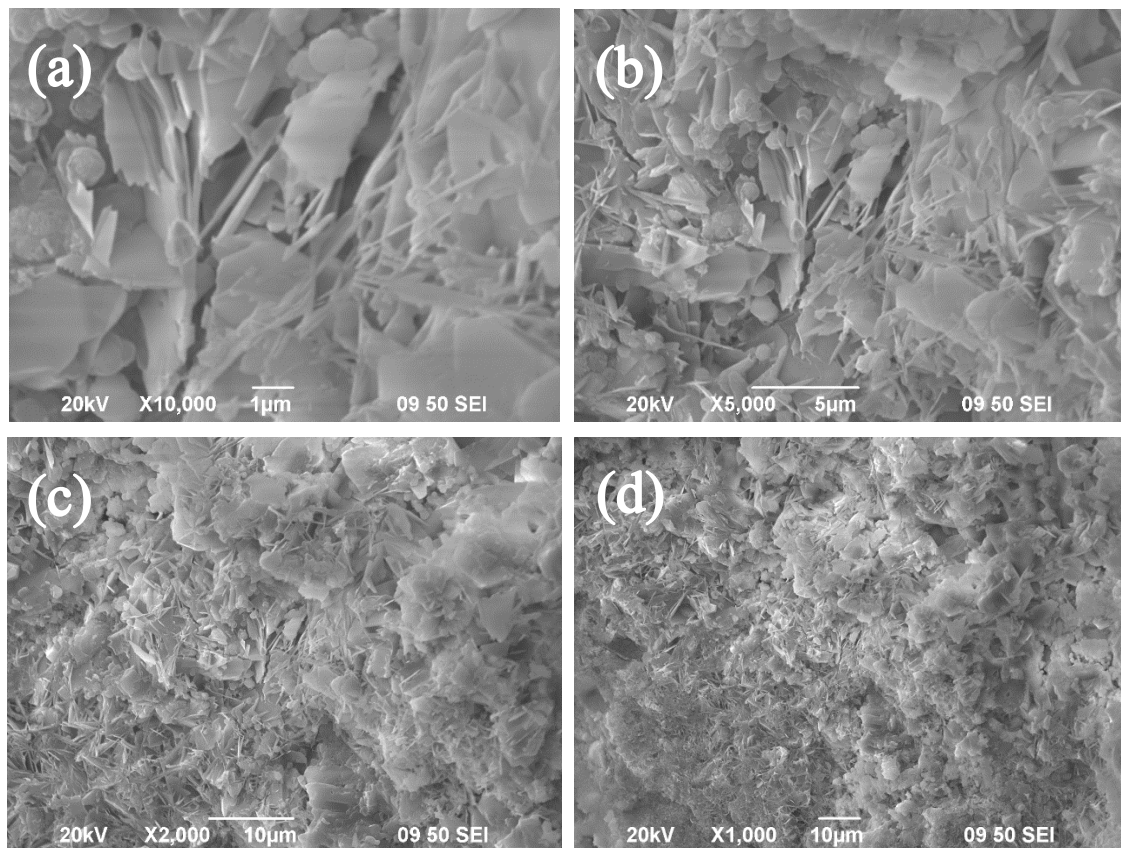


Figure 2. SEM photographs of the aerated brick at different magnifications: (a) $\times 10000$; (b) $\times 5000$; (c) $\times 2000$; (d) $\times 1000$.

To address the issue of water invasion of the aerated bricks, creating a water-repellent surface is an effective way, by modifying the surface with micro- and nanostructure and nanomaterials. Learning from the lotus effect, a hierarchical double structure, consisting of a characteristic epidermis equipped with micrometer-sized papilla arrays and the covering waxes [13,15], significantly reduces the contact area and the adhesion force between water droplets and the surface, thus enables the water repellency of the surface.

As shown in the schematic diagram in Figure 3, homemade highly dispersive TiO_2 nanoparticles were employed to coat on the aerated brick surface by dip coating method, creating a rough epidermis of the surface with TiO_2 nanoparticle clusters. On the other hand, the TiO_2 nanoparticles clad with TEOS undergo hydrolysis, forming $-\text{OH}$ terminal groups on the surface. At the same time, the $-\text{Si}-\text{OH}$ groups in the hydrolyzed PFOTS are dehydrated with the $-\text{OH}$ group on the TiO_2 surface by means of a self-assembling process and eventually build the hierarchical architecture. According to the Cassie-Baxter wetting model [18], this artificial highly textured surface modified with super-hydrophobic groups is responsible for water repellency, holding great potential for self-cleaning and water-proofing applications [19–21].

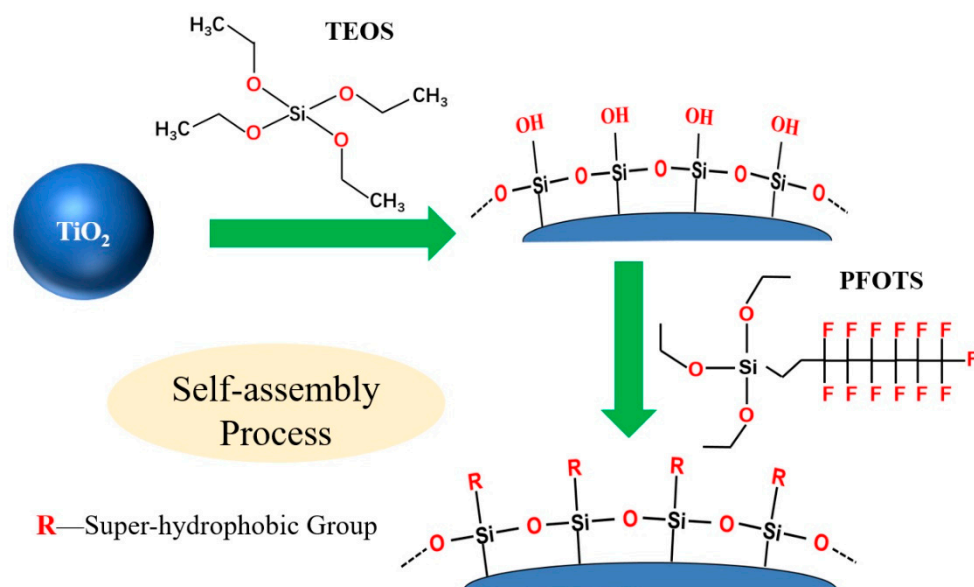


Figure 3. Schematic diagram of the surface modification.

The highly dispersive TiO_2 nanoparticles in water were prepared, enabling the preparation of environmentally friendly aqueous based suspension. Being a wide gap semiconductor [22,23] and nontoxic material, TiO_2 has been extensively used in areas of solar cells [23], photocatalysis [1], whitening, and ultraviolet shielding. The crystal phase of the prepared TiO_2 was revealed by XRD (Figure S2 in the Supplementary Materials). The diffraction peaks located at 25.2° , 37.7° , 48.0° , 53.9° , 62.6° were well indexed to its (101), (004), (200), (105) and (204) reflections respectively (JCPDS Card Number 21-1272), indicating anatase crystal structure of TiO_2 [1]. The dispersion characteristic of TiO_2 , which can be evaluated by the degree of nanoparticles aggregation in water, is of crucial importance to the aqueous based suspension fabrication. As shown in Figure 4, the median size of secondary particles is about $0.28 \mu\text{m}$, and the narrow distribution ranging between 0.1 and $0.6 \mu\text{m}$ implies a high degree of dispersion for the prepared TiO_2 in water.

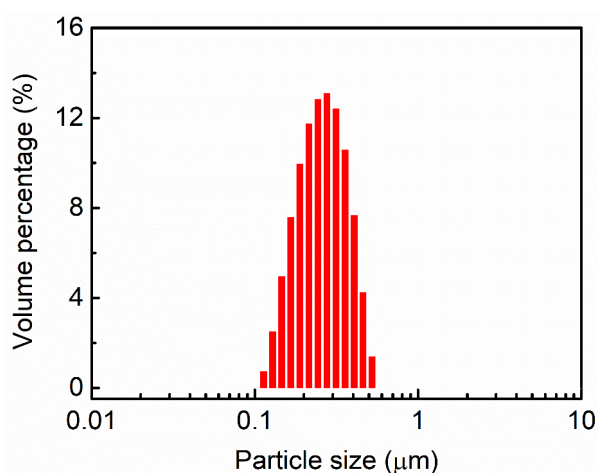


Figure 4. Particle size distribution of TiO_2 dispersed in water.

The surface morphology of the TiO_2 nanoparticles with super-hydrophobic modification coated on a silicon wafer is visualized in Figure 5. From the AFM topographic image and the sectional view of the height variation, it is estimated that the diameter of a single TiO_2 particle is about 50 nm on average, while the clusters range on the sub micrometer scale, in agreement with the secondary particle size distribution presented in Figure 4. The aerated brick was dipped into the TiO_2 based aqueous

super-hydrophobic suspension, introducing the micro- and nanostructure on the outmost surface of the brick. Along with the micrometer-sized pores in the brick, a certain rough surface modified with super-hydrophobic groups was built, as shown in Figure S3 in the Supplementary Materials.

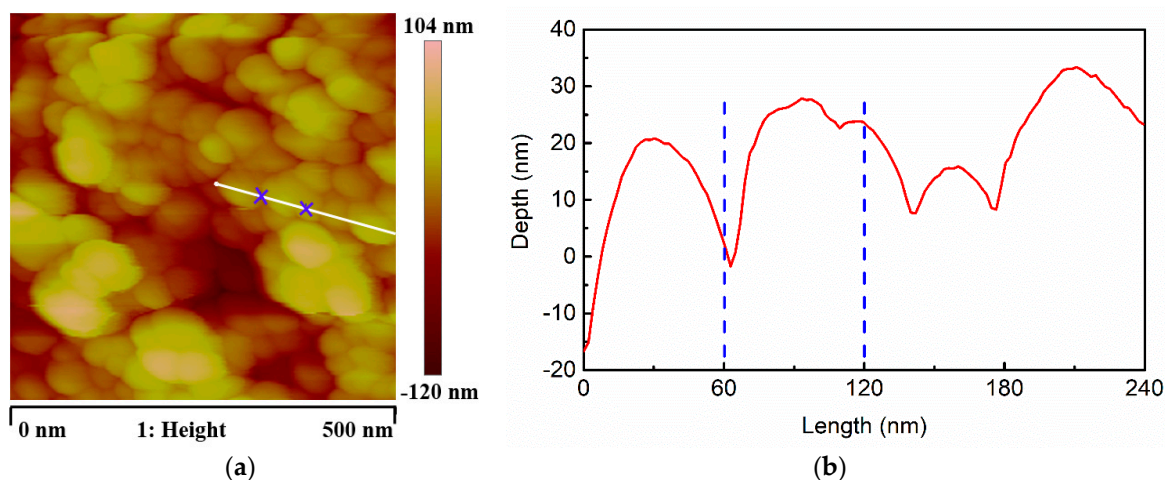


Figure 5. AFM image of TiO₂ based aqueous super-hydrophobic suspension coated on a silicon wafer: (a) Top view; (b) Sectional height difference along the white line in (a).

As displayed in Figure 6, FT-IR was employed to characterize the functional groups and the molecular bonding in the modified TiO₂ nanoparticles with PFOTS. The upper blue curve in Figure 6 shows the absorption peaks of PFOTS (including TEOS), in which the existence of C-F bonds in the form of CF, CF₂ and CF₃ are situated at 520, 739, 954, 1120 and 1205 cm⁻¹ [24]. The peaks at 1078 cm⁻¹ and 800 cm⁻¹ are associated with the asymmetric stretching vibration and bending mode of Si-O-Si bonds formed by dehydrate reaction of the silane coupling agent, respectively [25,26]. The peak located at 897 cm⁻¹ is assigned to the C-H bonds [25,26]. The Si-O-C bond appears at 1142 cm⁻¹, which confirms that the functional groups from PFOTS are linked to the silica network [27].

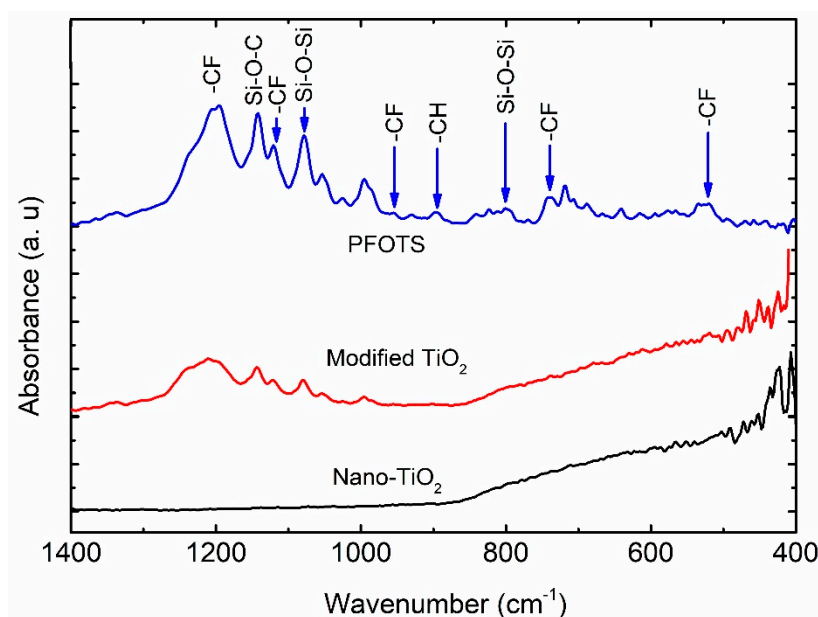


Figure 6. FT-IR spectra of the PFOTS modified nano-TiO₂ particles.

The middle red curve in Figure 6 shows the infrared absorption of the PFOTS modified nano-TiO₂, while the bottom black line gives the spectrum of nano-TiO₂ before treatment. It can clearly be seen

that the middle spectrum is a superposition of the upper and bottom ones, which implies that the PFOTS is attached to the TiO_2 nanoparticles.

The hydrophobicity of the surface can be determined by its contact angle. As displayed in Figure 7, a contact angle of 146° on average demonstrates an excellent water-repellency performance of the aerated brick surface with hierarchical structure and super-hydrophobic material modification.

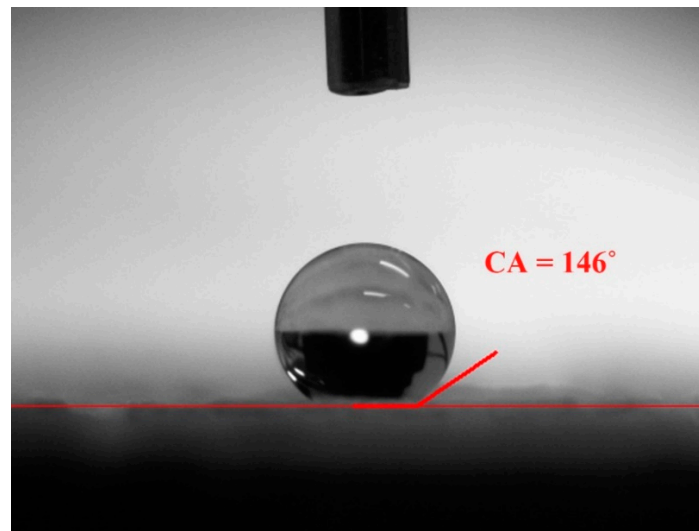


Figure 7. Contact angle test of the hydrophobic surface.

To further investigate the water-proofing performance of the bricks with a hydrophobic surface, a water immersion experiment was carried out, as shown in Figure 8. The sample with surface modification is shown in the left in Figure 8a,b), while the right in Figure 8a,b displays the bare brick. It is apparently observed that the brick with surface modification was floating on the water like a boat, while the control brick sank to the bottom of the water. The water-repellent surface dams the water into the pores of the brick, shielding the porous interior and forming relatively lower density than that of the water. By contrast, the water can easily permeate into the bare brick through the pores. To be more specific, the weight variations of the two brick samples were recorded before and after immersed into the water. A weight increment of 55.1% was detected for the bare brick after 24 h immersion, as shown in Figure 9. On the other hand, the weight of the brick with surface modification showed a small increase of about 4.3%, implying an excellent water resistance. This water immersion test preliminarily demonstrated the water proofing performance of the super-hydrophobic coating on the aerated bricks. Further investigation on the aging test and weather fastness would be carried out to encourage the widespread application.



Figure 8. Water immersion experiment of the aerated bricks w/o surface modification: (a) Side view; (b) Top view.

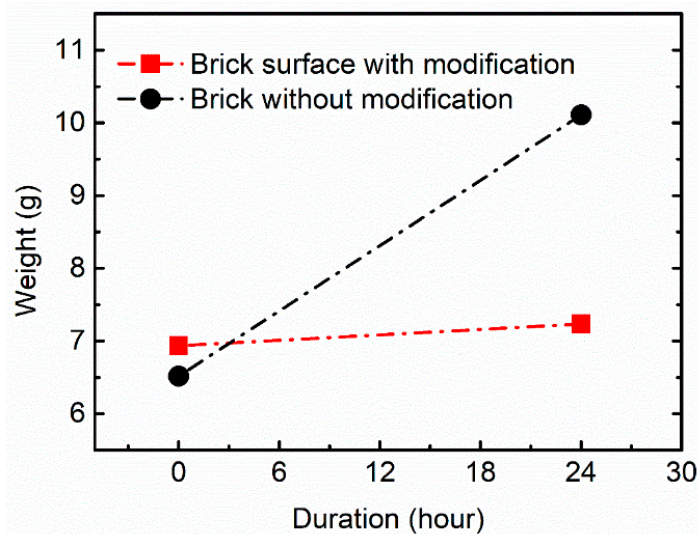


Figure 9. Comparison of weight increment between the bricks w/o surface modification immersed in water.

The highly dispersive TiO₂ nanoparticles modified with super-hydrophobic agent were prepared as aqueous based suspension, which is coated onto the aerated brick to create water-repellent surface. This property could effectively prevent the aerated bricks made of stone powder waste from rainwater invasion and corrosion, maintaining the outstanding performance of the bricks and keeping fresh appearance of the buildings. Tailoring the aerated brick to the water-proofing needs by utilizing nanomaterials in an environmentally friendly way introduces a new strategy for waste recycling and enlarges the application scale of super-hydrophobic technology.

4. Conclusions

In this study, the stone powder waste from stone processing was recycled into aerated bricks, which possess a pore structure that makes them prone to rainwater erosion. In order to block the outside water and make sure the bricks keep their edge, a strategy of making the brick surface water-repellent was introduced. Homemade highly dispersive TiO₂ nanoparticles modified with hydrophobic groups deriving from PFOTS were prepared as an aqueous suspension. It is coated onto the aerated brick by means of a dip coating method, creating a super-hydrophobic surface. The contact angle for water droplet on the surface reached 146°, indicating exceptional water-proofing performance. Compared to an increase by 55.1% in weight for a bare brick immersed in water for 24 h, negligible water absorption for the brick with surface modification also practically verified the outstanding water repellency and the effectiveness. This approach opens up the possibility of applying nanomaterials and technologies to improve the performances of products from waste recycling, and expands the application scope of the prepared aqueous based hydrophobic coating.

Supplementary Materials: The following are available online at <http://www.mdpi.com/2076-3417/9/13/2619/s1>, Figure S1: Images of EDS detected area of (a) the stone powder and (b) aerated brick, Figure S2: XRD pattern of TiO₂ nanoparticles, Figure S3: SEM image of the aerated brick surface with modification, Table S1: Elemental composition of the sample in Figure S1(a), Table S2: Elemental composition of the sample in Figure S1(b).

Author Contributions: Conceptualization, T.L. and S.Z.; methodology, H.Z. and S.W.; validation, Y.J., B.S. and Z.W.; formal analysis, T.L., B.S. and S.W.; investigation, S.Z., Y.J. and Z.W.; resources, S.Z., Y.J. and B.S.; data curation, H.Z. and S.W.; writing—original draft preparation, T.L., S.Z., H.Z. and S.W.; writing—review and editing, H.Z. and S.W.; supervision, S.W.

Funding: This research received no external funding.

Conflicts of Interest: The authors declare no conflict of interest.

References

1. Ji, Y.X.; Rong, X.; Zhong, H.; Wang, Y.H.; Wang, S.F.; Lu, L. Making Marble Powder Waste Profitable by Using Nano-TiO₂ Surface Modification for Air Quality Improvement Applications. *J. Nanomater.* **2017**, *2017*, 6501793. [[CrossRef](#)]
2. Aliabdo, A.A.; Abd Elmoaty, A.E.M.; Auda, E.M. Re-use of waste marble dust in the production of cement and concrete. *Constr. Build. Mater.* **2014**, *50*, 28–41. [[CrossRef](#)]
3. Ergün, A. Effects of the usage of diatomite and waste marble powder as partial replacement of cement on the mechanical properties of concrete. *Constr. Build. Mater.* **2011**, *25*, 806–812. [[CrossRef](#)]
4. Bilgin, N.; Yeprem, H.A.; Arslan, S.; Bilgin, A.; Günay, E.; Maroglu, M. Use of waste marble powder in brick industry. *Constr. Build. Mater.* **2012**, *29*, 449–457. [[CrossRef](#)]
5. Hebhouh, H.; Aoun, H.; Belachia, M.; Houari, H.; Ghorbel, E. Use of waste marble aggregates in concrete. *Constr. Build. Mater.* **2011**, *25*, 1167–1171. [[CrossRef](#)]
6. Wong, Y.; Tong, L.; Hu, Y.; Wu, P. A self-assembly and high robustness super-hydrophobic coating based on waste marble powder. *Mater. Trans.* **2016**, *57*, 2127–2131. [[CrossRef](#)]
7. Mostafa, N.Y. Influence of air-cooled slag on physicochemical properties of autoclaved aerated concrete. *Cem. Concr. Res.* **2005**, *35*, 1349–1357. [[CrossRef](#)]
8. Huang, X.Y.; Ni, W.; Cui, W.H.; Wang, Z.J.; Zhu, L.P. Preparation of autoclaved aerated concrete using copper tailings and blast furnace slag. *Constr. Build. Mater.* **2012**, *27*, 1–5. [[CrossRef](#)]
9. Aulakh, D.S.; Singh, J.; Kumar, S. The Effect of Utilizing Rice Husk Ash on Some Properties of Concrete—A Review. *Curr. World Environ.* **2018**, *13*, 224–231. [[CrossRef](#)]
10. Zheng, D.D.; Ji, T.; Wang, C.Q.; Sun, C.J.; Lin, X.J.; Hossain, K.M.A. Effect of the combination of fly ash and silica fume on water resistance of Magnesium–Potassium Phosphate Cement. *Constr. Build. Mater.* **2016**, *106*, 415–421. [[CrossRef](#)]
11. Johnson R.E., Jr.; Dettre, R.H. Contact Angle Hysteresis. III. Study of an Idealized Heterogeneous Surface. *J. Phys. Chem.* **1964**, *68*, 1744–1750. [[CrossRef](#)]
12. Barthlott, W.; Ehler, N. *Raster-Elektronenmikroskopie der Epidermis-Oberflächen von Spermatoxyten*; Akademie der Wissenschaften und der Literatur: Mainz, Germany, 1977.
13. Lu, Y.; Sathasivam, S.; Song, J.L.; Crick, C.R.; Carmalt, C.J.; Parkin, I.P. Robust self-cleaning surfaces that function when exposed to either air or oil. *Science* **2015**, *347*, 1132–1135. [[CrossRef](#)] [[PubMed](#)]
14. Manabe, K.; Nishizawa, S.; Kyung, K.H.; Shiratori, S. Optical Phenomena and Antifrosting Property on Biomimetics Slippery Fluid-Infused Antireflective Films via Layer-by-Layer Comparison with Superhydrophobic and Antireflective Films. *Appl. Mater. Interfaces* **2014**, *6*, 13985–13993. [[CrossRef](#)] [[PubMed](#)]
15. Barthlott, W.; Mail, M.; Bhushan, B.; Koch, K. Plant Surfaces: Structures and Functions for Biomimetic Innovations. *Nano-Micro Lett.* **2017**, *9*, 23. [[CrossRef](#)] [[PubMed](#)]
16. Zhong, H.; Hu, Y.; Wang, Y.H.; Yang, H.X. TiO₂/silane coupling agent composed of two layers structure: A super-hydrophilic self-cleaning coating applied in PV panels. *Appl. Energy* **2017**, *204*, 932–938. [[CrossRef](#)]
17. Lakhani, R.; Kumar, R.; Tomar, P. Utilization of Stone Waste in the Development of Value Added Products: A State of the Art Review. *J. Eng. Sci. Technol. Rev.* **2014**, *7*, 180–187. [[CrossRef](#)]
18. Cassie, A.B.D.; Baxter, S. Wettability of Porous Surfaces. *Trans. Faraday Soc.* **1944**, *40*, 546–551. [[CrossRef](#)]
19. Suzuki, S.; Ueno, K. Apparent Contact Angle Calculated from a Water Repellent Model with Pinning Effect. *Langmuir* **2017**, *33*, 138–143. [[CrossRef](#)]
20. Simpson, J.T.; Hunter, S.R.; Aytug, T. Superhydrophobic Materials and Coatings: A Review. *Rep. Prog. Phys.* **2015**, *78*, 086501. [[CrossRef](#)]
21. Cao, M.; Guo, D.; Yu, C.; Li, K.; Liu, M.; Jiang, L. Water-Repellent Properties of Superhydrophobic and Lubricant-Infused “Slippery” Surfaces: A Brief Study on the Functions and Applications. *ACS Appl. Mater. Interfaces* **2016**, *86*, 3615–3623. [[CrossRef](#)]
22. Wang, S.F.; Fong, W.K.; Wang, W.; Surya, C. Growth of highly textured SnS on mica using an SnSe buffer layer. *Thin Solid Films* **2014**, *564*, 206–212. [[CrossRef](#)]
23. Wang, S.F.; Wang, W.; Fong, W.K.; Yu, Y.; Surya, C. Tin Compensation for the SnS Based Optoelectronic Devices. *Sci. Rep.* **2017**, *7*, 39704. [[CrossRef](#)] [[PubMed](#)]

24. Hozumi, A.; Takai, O. Effect of hydrolysis groups in fluoro-alkyl silanes on water repellency of transparent two-layer hard-coatings. *Appl. Surf. Sci.* **1996**, *103*, 431–441. [[CrossRef](#)]
25. Latthe, S.S.; Imai, H.; Ganesan, V.; Rao, A.V. Superhydrophobic silica films by sol-gel co-precursor method. *Appl. Surf. Sci.* **2009**, *256*, 217–222. [[CrossRef](#)]
26. Teshima, K.; Sugimura, H.; Inoue, Y.; Takai, O. Gas barrier performance of surface-modified silica films with grafted organosilane molecules. *Langmuir* **2003**, *19*, 8331–8334. [[CrossRef](#)]
27. Brassard, J.-D.; Sarkar, D.K.; Perron, J. Synthesis of monodisperse fluorinated silica nanoparticles and their superhydrophobic thin films. *ACS Appl. Mater. Interfaces* **2011**, *3*, 3583–3588. [[CrossRef](#)] [[PubMed](#)]



© 2019 by the authors. Licensee MDPI, Basel, Switzerland. This article is an open access article distributed under the terms and conditions of the Creative Commons Attribution (CC BY) license (<http://creativecommons.org/licenses/by/4.0/>).